ARTICLE
Journal of Cellular Biochemistry 113:2567–2575 (2012)

Journal of Cellular Biochemistry

Novel Polypyridyl Chelators Deplete Cellular Zinc and Destabilize the X-Linked Inhibitor of Apoptosis Protein (XIAP) Prior to Induction of Apoptosis in Human Prostate and Breast Cancer Cells

Jian Zuo,[1,2] Sara M. Schmitt,[1] Zhen Zhang,[1,2] Jai Prakash,[3] Yuhua Fan,[2] Caifeng Bi,[2] Jeremy J. Kodanko,[3**] and Q. Ping Dou[1*]

[1] *Developmental Therapeutics Program, Barbara Ann Karmanos Cancer Institute, Departments of Oncology, Pharmacology and Pathology, School of Medicine, Wayne State University, Detroit, Michigan 48201*

[2] *Key Laboratory of Marine Chemistry Engineering and Technology, Ministry of Education, College of Chemistry and Chemical Engineering, Ocean University of China, Qingdao 266100, People's Republic of China*

[3] *Department of Chemistry, Wayne State University, Detroit, Michigan 48202*

ABSTRACT

X-linked inhibitor of apoptosis protein (XIAP), inhibits the initiation and execution phases of the apoptotic pathway. XIAP is the most potent member of the inhibitor of apoptosis protein (IAP) family of the endogenous caspase inhibitors. Therefore, targeting XIAP may be a promising strategy for the treatment of apoptosis-resistant malignancies. In this study, we systematically studied the relationships of chemical structures of several novel ligands to their zinc (Zn)-binding ability, molecular target XIAP, and tumor cell death-inducing activity. We show that treatment of PC-3 prostate cancer and MDA-MB-231 breast cancer cells with these membrane-permeable Zn-chelators with different Zn affinities results in varying degrees of XIAP depletion. Following decreased level of XIAP expression, we also show apoptosis-related caspase activation and cellular morphological changes upon treatment with strong Zn-chelators N4Py and BnTPEN. Addition of Zn has a full protective effect on the cells treated with these chelators, while iron (Fe) addition has only partial protection that, however, can be further increased to a comparable level of protection as Zn by inhibition of ROS generation, indicating that cell death effects mediated by Fe- but not Zn-complexes involve redox cycling. These findings suggest that strong Zn-chelating agents may be useful in the treatment of apoptosis-resistant human cancers. J. Cell. Biochem. 113: 2567–2575, 2012.

KEY WORDS: XIAP; POLYPYRIDYL CHELATOR; ZINC; APOPTOSIS; PROSTATE CANCER; BREAST CANCER

The X-linked inhibitor of apoptosis (XIAP), has recently received considerable attention due to its ability to directly inhibit both initiation and execution phases of the caspase cascade. XIAP is a member of the inhibitor of apoptosis protein (IAP) family, which selectively binds and inhibits caspases [Eckelman et al., 2006]. All IAPs contain 1–3 baculoviral IAP repeat (BIR) motifs, which are cysteine and histidine rich and can fold into functionally independent structures that bind zinc (Zn). These domains contain tails derived from amino-terminal "linker" regions, which are important to IAP function [Liston et al., 2003]. Many IAPs also contain RING finger Zn-binding domains, which have E3 ligase activity as well as caspase activation and recruitment (CARD)

J. Zuo and S. Schmitt contributed equally to this study.

No potential conflicts of interest are reported.

Grant sponsor: Karmanos Cancer Institute 2009 Pilot Project Funding; Grant sponsor: National Cancer Institute; Grant numbers: 1R01CA120009, 3R01CA120009-04S1, 5R01CA127258-05.

*Correspondence to: Q. Ping Dou, The Developmental Therapeutics Program, Barbara Ann Karmanos Cancer Institute, Department of Oncology, School of Medicine, Wayne State University, 540.1 HWCRC, 4100 John R Road, Detroit, MI 48201. E-mail: doup@karmanos.org

**Correspondence to: Jeremy J. Kodanko, Department of Chemistry, Wayne State University, Detroit, MI 48202. E-mail: jkodanko@chem.wayne.edu

Manuscript Received: 24 January 2012; Manuscript Accepted: 6 March 2012

Accepted manuscript online in Wiley Online Library (wileyonlinelibrary.com): 13 March 2012

DOI 10.1002/jcb.24132 • © 2012 Wiley Periodicals, Inc.

domains [Yang et al., 2000; Schimmer and Dalili, 2005]. XIAP contains three BIR motifs and a carboxy-terminal RING finger domain [Rothe et al., 1995; Duckett et al., 1996; Liston et al., 1996; Uren et al., 1996]. The BIR2 domain of XIAP can interact with the amino terminal end of the small subunit of caspase-7, stabilizing the interaction of the linker in the catalytic groove and causing its inhibition [Suzuki et al., 2001a], while the linker region accounts entirely for the inhibition of caspase-3 [Chai et al., 2001; Huang et al., 2001]. The BIR3 domain directly binds to, and inhibits caspase-9 through an amino-terminal end created by caspase-9 self-cleavage [Liston et al., 2003; Shiozaki et al., 2003] while the BIR1 domain displays no inhibitory activity. Importantly, the E3 ligase activity of the RING finger domain may allow XIAP to trigger ubiquitination of caspases-3 and -7, a process that represents one of the potential anti-apoptotic mechanisms of XIAP [Huang et al., 2000; Suzuki et al., 2001b].

Because many cancers exhibit decreased levels of apoptosis, it is no surprise that XIAP levels are elevated in many cancer cell lines and that cancer cells are sensitized to chemotherapeutics by suppression of XIAP protein [Schimmer et al., 2006]. Additionally, Zn is very important to the development and progression of both normal and malignant cells [Provinciali et al., 1995; Chang et al., 2006; Murakami and Hirano, 2008; Franklin and Costello, 2009]. Zn-binding within the RING finger domain of XIAP is critical to the function of the enzyme [Sun et al., 2000]. Therefore, chelation of Zn from the binding domain of XIAP may be a viable strategy for targeting the enzyme.

In the current study, we show that the treatment of human prostate (PC-3) and breast (MDA-MB-231) cancer cells with several novel polypyridyl chelators induces rapid depletion of XIAP protein. Early XIAP depletion is followed by later apoptosis-specific caspase-3 activation, poly(ADP-ribose) polymerase (PARP) cleavage and cellular morphological changes. These cellular results are approximately correlated with the order of the strengths of Zn binding for polypyridyl chelators measured in solutions, and can be reversed by addition of Zn. Addition of iron (Fe), however, has differential effects, which may be due to generation of ROS. These important results suggest that some chelators may have modes of action involving Fe.

MATERIALS AND METHODS

COMPOUNDS

Compounds BnTPEN [Duelund et al., 2001], N4Py [Roelfes et al., 1997], TPEN [Tang et al., 2006], DPA [Wong et al., 2010], and TPA [Britovsek et al., 2005] were synthesized, according to the methods in the indicated publications, in the Kodanko laboratory (Wayne State University, Detroit, MI). $ZnCl_2$, $Fe(ClO_4)_2 \cdot H_2O$ and *N*-acetylcysteine (NAC) were purchased from Sigma–Aldrich (St. Louis, MO). Compounds were dissolved in DMSO (Sigma–Aldrich) at stock concentrations of 50 mM and stored at $-20^{\circ}C$.

ZINC DISSOCIATION CONSTANTS

Zinc dissociation constants (Kds) for DPA, TPA, and TPEN are literature values determined in aqueous solution (0.1 M KNO_3) [Anderegg et al., 1977], and Zn Kds for BnTPEN and N4Py (see Table in Fig. 1) were determined spectrophotometrically by the competition method as previously described [Jackson and Kodanko, 2010]. Values were calculated relative to Fe^{II} using equimolar chelator, $ZnCl_2$, and $FeCl_2$.

CELL CULTURE AND WHOLE CELL EXTRACT PREPARATION

Human prostate (PC-3) and breast (MDA-MB-231) cancer cells, purchased from American Type Culture Collection (Manassas, VA),

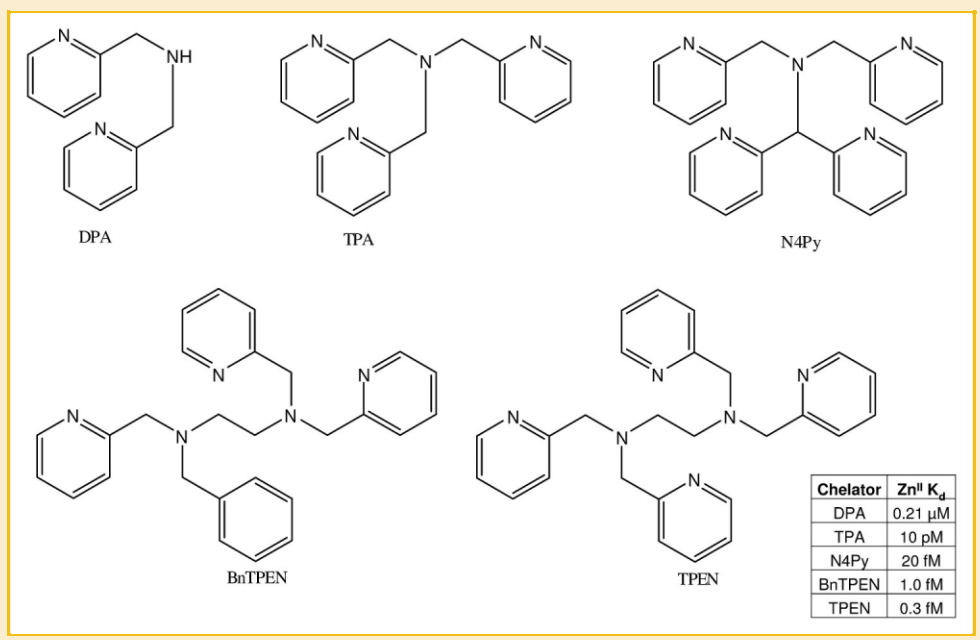

Chelator	Zn^{II} K_d
DPA	0.21 μM
TPA	10 pM
N4Py	20 fM
BnTPEN	1.0 fM
TPEN	0.3 fM

Fig. 1. Structures and Zn-binding affinities (Zn^{II} K_d) of tested chelators.

were cultured in RPMI-1640 (PC-3) and DMEM/F-12 (MDA-MB-231) media, respectively, supplemented with 10% fetal bovine serum (FBS), 100 U/ml penicillin and 100 μg/ml streptomycin (Life Technology, Carlsbad, CA). Cells were maintained in an atmosphere containing 5% CO_2 at a temperature of 37°C. Whole cell extracts were prepared as previously described [An et al., 1998]. Briefly, cells were washed twice with phosphate-buffered saline and lysed in a whole cell lysis buffer (50 mM Tris–HCl, pH 8.0, 150 mM NaCl, 0.5% NP40). The mixtures were then vortexed for 20 min at 4°C and centrifuged at 12,000 rpm for 12 min. Supernatants were collected as whole cell extracts and used for Western blot analysis.

CELL VIABILITY ASSAY

The MTT (3-(4,5-dimethylthiazol-2-yl)-2,5-diphenyltetrazolium bromide) assay was used to measure effects of the compounds or compound–metal (Fe, Zn) mixtures on prostate or breast cancer cell viability. Cells were plated in 96-well plates and grown to 70–80% confluency, followed by addition of each compound or compound–metal mixture at the indicated concentrations (Fe and Zn alone = 10 or 100 μM; N4Py and BnTPEN alone = 1, 2.5, 5, 10, or 15 μM and in combination with metals = 5 or 10 μM; DPA, TPA, and TPEN = 1, 2.5, 5, 10, or 15 μM) for 20, 24, or 48 h. MTT (1 mg/ml) in PBS was then added to wells and incubated at 37°C for 3 h to allow for complete cleavage of the formazan salt by viable cells. MTT was then removed and 100 μl DMSO was added, followed by colorimetric analysis using a Victor3 multilabel plate reader (PerkinElmer, Wellesley, MA) at an absorbance of 560 nm. Absorbance values plotted were the mean from triplicate experiments.

WESTERN BLOT ANALYSIS

PC-3 or MDA-MB-231 cells were treated as indicated in the figure legends and lysed as described above. Protein concentrations of whole cell lysates were determined using the Bio-Rad Protein Assay (Bio-Rad, Hercules, CA). Cell lysates (40 μg) were separated by sodium dodecylsulfate–polyacrylamide gel electrophoresis (SDS–PAGE) and transferred to nitrocellulose membrane, followed by incubation with indicated primary (PARP; Enzo Life Sciences, Farmingdale, NY; XIAP, actin; Santa Cruz Biotechnology, Santa Cruz, CA; and cleaved caspase-3; Cell Signaling, Danvers, MA) and secondary antibodies (Bio-Rad) and visualization using enhanced chemiluminescence reagent (Denville Scientific, Metuchen, NJ) as previously described [Chen et al., 2005].

CASPASE-3 ACTIVITY ASSAY

Caspase-3 activity was determined by release of AMC groups from a caspase-3-specific substrate, Ac-DEVD-AMC. Briefly, cells were treated with each compound as indicated in the figure legends, followed by preparation of whole cell lysates. The cell lysates (25 μg) were then incubated in 100 μl assay buffer (20 mM Tris–HCl, pH 7.5) with 40 μM caspase-3 substrate in a 96-well plate. The reaction mixture was incubated at 37°C for 2.5 h, followed by measurement of hydrolyzed AMC groups using a Victor3 multilabel plate reader (PerkinElmer) with an excitation filter of 380 nm and an emission filter of 460 nm.

MORPHOLOGICAL CHANGES

Cellular changes in morphology were observed before and after each treatment using a Zeiss Axiovert 25 microscope (Thornwood, FL). Rounded and detached cells were considered dead.

RESULTS

STRUCTURES AND ZINC BINDING AFFINITY OF POLYPYRIDYL LIGANDS DETERMINED UNDER CELL-FREE CONDITIONS

Several unique, cell-permeable (see below) nitrogen-containing polypyridyl ligands (Fig. 1) have varying denticity, from three for DPA to six for TPEN. These ligands can bind to metal ions, such as Fe, Zn, or Cu to form stable metal complexes [Anderegg et al., 1977] with different binding affinities. The structure and biological activity relationship of these ligands have never been systematically investigated. We therefore first determined and compared the Zn-binding affinity of these ligands in solutions, and found that the rank of their Zn-binding affinity under cell-free conditions was: TPEN > BnTPEN > N4Py > TPA > DPA (see Table in Fig. 1). We then determined the relationship of the Zn-binding strengths and biological activities of these ligands in intact human cancer cells.

INHIBITION OF PROSTATE CANCER CELL VIABILITY AND INDUCTION OF APOPTOSIS BY THE TESTED POLYPYRIDYL CHELATORS ARE ASSOCIATED WITH DEPLETION OF XIAP

XIAP uses Zn^{II} ion as a cofactor and therefore, the cellular Zn-binding ability of these ligands can be exploited by measuring effect on levels of XIAP protein expression. We then determined whether these Zn chelators could remove Zn from XIAP protein, causing its degradation and leading to cell death and growth inhibition and whether the rank of biological activities of these ligands in cultured cancer cells matches that found in solutions. TPEN and TPA are known to be cell permeable [Hashemi et al., 2007; Ghosh et al., 2010]. Because N4Py and BnTPEN show similar chemical structure and biological activity to TPEN (vide infra), they should be cell permeable, too.

To determine the effect of these chelators on cell viability, human prostate cancer PC-3 cells were treated with each of the selected agent at 1, 2.5, or 5 μmol/L or with DMSO as a solvent control for 24 h, followed by performance of MTT assay (see Materials and Methods Section for details; Fig. 2A). Cells treated with TPEN, BnTPEN, N4Py, and TPA at 5 μmol/L exhibited dramatically decreased cell viability (about 100%, 100%, 90%, and 90%, respectively). When cells were treated with 2.5 μmol/L of TPEN, BnTPEN, N4Py, and TPA, cell viability was reduced by about 70%, 90%, 20%, and 15%, respectively (Fig. 2A), which roughly matched the rank of their Zn-binding strengths found in solutions (Fig. 1). The slightly different relative potency of these ligands between solutions and cells might be due to different stability and permeability. All of these ligands at 1 μmol/L had no inhibitory effect (Fig. 2A). Treatment with DPA even at 5 μmol/L resulted in no inhibition of cellular viability (Fig. 2A). Therefore, the ability of these ligands to inhibit cellular viability appears to correspond to their Zn-binding ability determined in solutions.

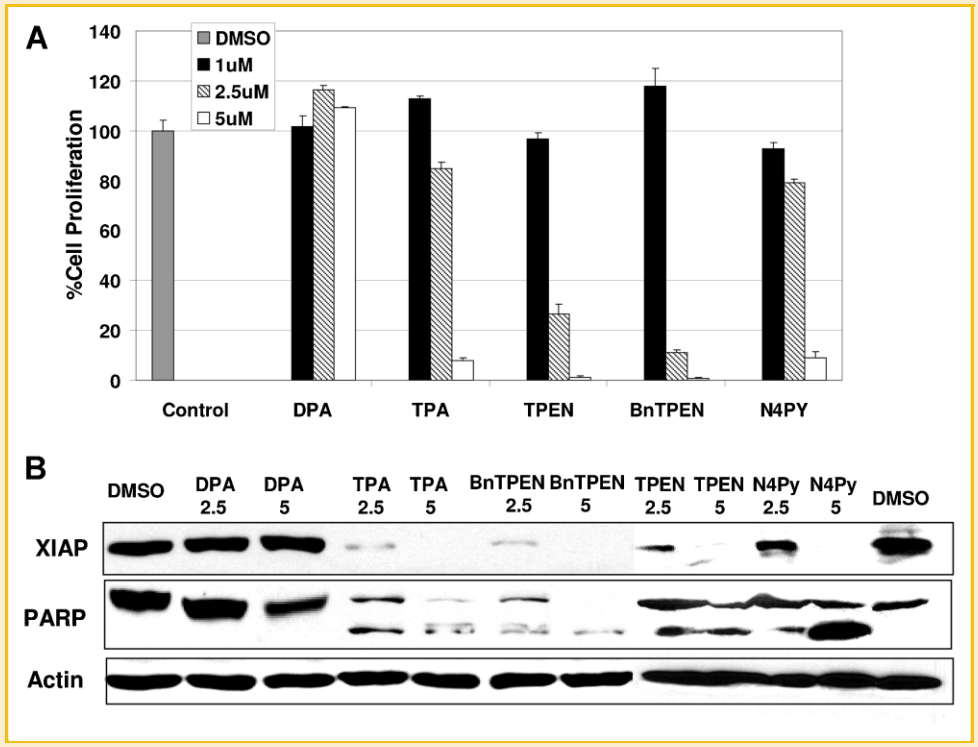

Fig. 2. Inhibition of prostate cancer PC-3 cell viability and induction of apoptosis is associated with XIAP depletion and dependent on Zn-binding affinity. A: MTT assay (24 h); B: Western blot analysis (16 h). The concentration of each compound used was 1, 2.5, or 5 μM, as indicated.

Additionally, to determine the effects of chelators on cancer cell death, Western blot analysis was performed on PC-3 cell lysates after 16 h treatment with 2.5 or 5 μmol/L of each chelator. Apoptosis-associated PARP cleavage was observed in cells treated for 16 h with all four ligands, TPEN, BnTPEN, N4Py, and TPA, at 5 μmol/L (Fig. 2B). Lower levels of PARP cleavage were observed when these compounds were used at 2.5 μmol/L (Fig. 2B). Again, we observed some slight change in relative potency of these ligands under cellular conditions compared to solution, which could be due to the difference in stability and permeability of these ligands and possible experimental errors. Importantly, associated with induction of apoptosis, depletion of XIAP was observed in cells treated with 2.5 μmol/L of TPEN, BnTPEN, N4Py and TPA, and XIAP was completely undetectable when these ligands were used at 5 μmol/L (Fig. 2B), suggesting that XIAP depletion is associated with the inhibition of cell proliferation and the induction of PARP cleavage and these effects are, at least partially dependent on Zn-binding affinities of the chelators. Again, DPA treatment neither generated PARP cleavage nor XIAP decrease (Fig. 2B).

INHIBITION OF CELL VIABILITY AND INDUCTION OF APOPTOSIS ASSOCIATED WITH XIAP DEPLETION ARE ALSO OBSERVED IN HUMAN BREAST CANCER CELLS

Similar effects were also observed in a second cell line, MDA-MB-231, which was derived from a human breast cancer patient. MDA-MB-231 cells were treated with the selected chelators at 10 and 15 μmol/L or with the solvent DMSO for 48 h, followed by measurement of cellular viability by MTT assay. We noted that the treatment time was longer for MDA-MB-231 cells than the PC-3 cells in order to see the inhibitory effect. TPA, TPEN, BnTPEN, and N4Py treatment resulted in inhibition of cellular viability, while DPA was again the least potent chelator, causing only 50% inhibition at 15 μmol/L (Fig. 3A). However, all four chelators (TPA, TPEN, BnTPEN, and N4Py) were much less potent in MDA-MB-231 cells, reaching a maximum of only 70–85% inhibition of viability at 15 μmol/L (Fig. 3A), than in PC-3 cells, where a maximum inhibition of nearly 100% was reached after treatment with only 5 μmol/L (Fig. 2A), which may suggest that this strategy may be more useful in treating prostate cancer than breast cancer.

Also similar to the results observed in PC-3 cells, Western blot analysis showed that 3 h treatment with 10 μmol/L of TPA, TPEN, BnTPEN, and N4Py induced depletion of full-length XIAP, with almost complete disappearance as a result of BnTPEN treatment (Fig. 3B). Following decreased levels of XIAP protein at 3 h, caspase-3 activation was detected after 24 h treatment with 10 μmol/L of TPA, TPEN, BnTPEN, and N4Py, evident by cleavage of caspase-3 into its active form (17 kDa; Fig. 3B) and induction of caspase-3 enzymatic activity (Fig. 3C). Because an antibody specific for the cleaved caspase-3 fragment (17 kDa) was used, no full-length caspase-3 bands (36 kDa) were detected. Maximum caspase activation occurred after 24 h treatment with TPA, TPEN, BnTPEN, and N4Py (approximately, 12-, 7-, 16- and 13-fold, respectively). This was also accompanied by decreased levels of full-length PARP protein and/or the appearance of PARP cleavage product after 24 h treatment (Fig. 3B). Little or no PARP cleavage was observed at 3 h (Fig. 3B), suggesting that apoptosis occurs after XIAP depletion. In

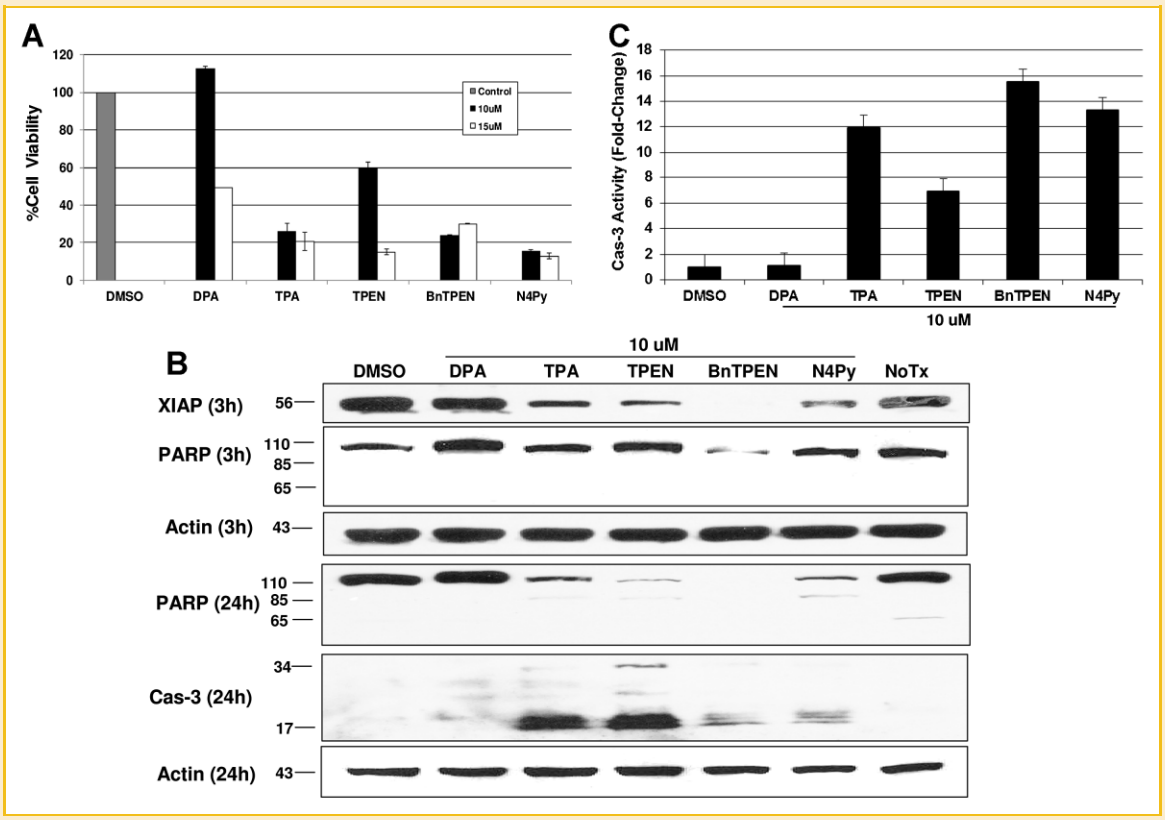

Fig. 3. Inhibition of breast cancer MDA-MB-231 cell viability and induction of apoptosis is associated with XIAP depletion and dependent on Zn-binding affinity. A: MTT assay (48 h); B: Western blot analysis (3 and 24 h); C: Caspase-3 activity assay (24 h). The concentrations of each compound used were 10 (A–C) or 15 μM (A).

contrast, treatment with DPA induced neither XIAP depletion at 3 h nor apoptosis at 24 h (Fig. 3B,C).

ADDITION OF Zn AND Fe HAS DIFFERENTIAL EFFECTS ON BnTPEN- AND N4Py-INDUCED CELL VIABILITY INHIBITION AND APOPTOSIS

To determine the effect of metal addition on BnTPEN- and N4Py-mediated inhibition of cell viability, PC-3 cells were treated with each chelator at 5 μmol/L in the absence or presence of Fe or Zn at various concentrations. Cell viability was subsequently measured by MTT assay (Fig. 4A). Addition of Zn at concentrations as low as 0.5 (data not shown) to 10 μmol/L reversed inhibition of cell growth by 5 μmol/L N4Py, but Fe, even at concentrations of 5 and 10 μmol/L exhibited little rescue of cellular viability (Fig. 4A). Also, addition of Zn at concentrations of 2.5 (data not shown) to 10 μmol/L, but not Fe even at concentrations as high as 10 μmol/L, reversed inhibition of cell growth by BnTPEN (Fig. 4B).

Similarly, Zn completely, while Fe partially reversed PARP cleavage induced by treatment with N4Py and BnTPEN, as found by Western blot analysis (Fig. 4C). XIAP depletion at 3 h by N4Py was reversed by both Fe and Zn, while XIAP depletion by BnTPEN was reversed completely with Zn, but only partially by Fe (Fig. 4C). As observed with cell viability assay and PARP cleavage, the morphological changes induced by both ligands were reversible only by Zn, but not Fe (Fig. 4D). Although Fe partially reversed PARP cleavage and XIAP depletion induced by both ligands, Fe addition did not prevent cells from undergoing cell death (Fig. 4D), consistent with its failure to rescue cells from growth inhibition mediated by the ligands (Fig. 4A), which may again be explained by the ligand binding to Fe and producing oxidative stress (see below). The ability of Fe to rescue XIAP depletion by N4Py, but only partially rescue that induced by BnTPEN is concordant with N4Py binding Fe rather than Zn. Inhibition of XIAP degradation upon Fe addition may partially contribute to decreased apoptosis (Fig. 4C).

PRE-TREATMENT WITH Zn, BUT NOT Fe, REVERSES THE EFFECTS OF BOTH N4Py AND BnTPEN

To determine if the time at which metal is added affects the reversal of chelator-mediated effects, PC-3 cells were first treated with 100 μmol/L of Fe or Zn for 48 h, followed by co-treatment with 10 μmol/L of N4Py or BnTPEN for an additional 3 or 20 h. MTT assay was then performed to measure cell viability (Fig. 5A). Cells pre-treated with Zn displayed increased viability compared to cells treated with either N4Py or BnTPEN alone (Fig. 5A). In contrast, the inhibition of growth by N4Py and BnTPEN was sustained in cells pre-treated with Fe (Fig. 5A). Western blot analysis showed that apoptosis-associated PARP cleavage by N4Py and BnTPEN could also be reversed by Zn but not Fe (Fig. 5B). Importantly, pre-treatment with Zn, but not Fe also had a protective effect against XIAP depletion and apoptosis-associated morphological changes mediated by both N4Py and BnTPEN (Fig. 5B,C).

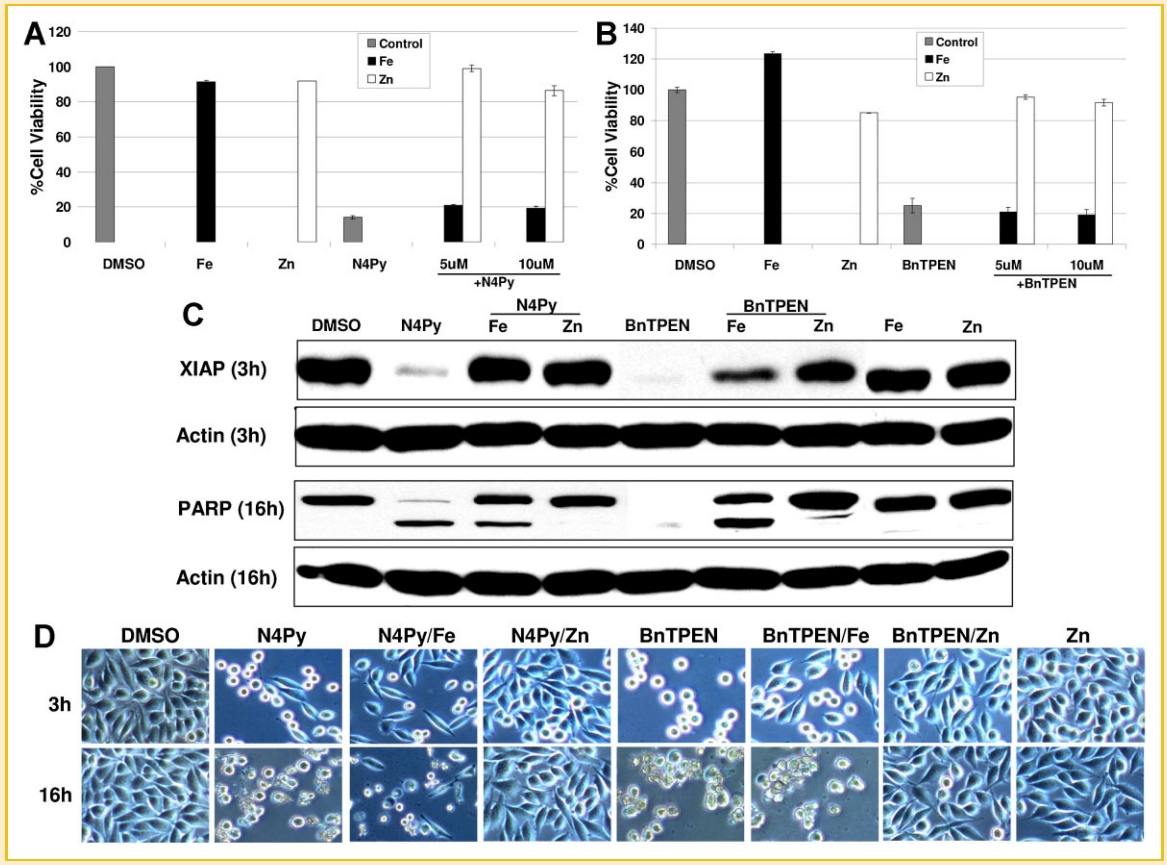

Fig. 4. Effect of metal addition on cell viability and apoptosis induction in PC-3 cells. A: MTT assay—Zn but not Fe reverses effect of N4Py on cell viability; B: MTT assay—only Zn is able to reverse effect of BnTPEN; concentrations and time points used for MTT assays: Fe and Zn alone = 10 μM, N4Py and BnTPEN alone, and in combination with metals = 5 μM, 24 h treatment; C: Western blot—Fe and Zn have different protective abilities to XIAP depletion induced by N4Py and BnTPEN. Fe partially rescues PARP cleavage by N4Py and BnTPEN while Zn completely reverses effects of both N4Py and BnTPEN; D: Zn, but not Fe, completely reverses morphological changes resulting from treatment with N4Py and BnTPEN. Treatment with iron (data not shown) resulted in similar effects as that with zinc. [Color figure can be seen in the online version of this article, available at http://wileyonlinelibrary.com/journal/jcb]

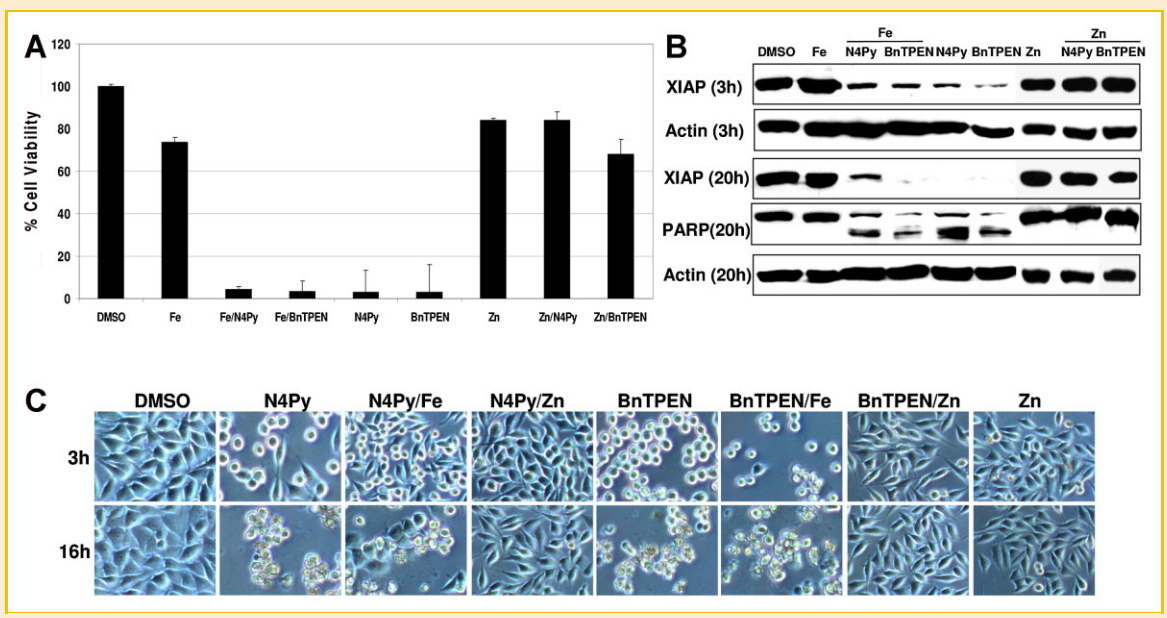

Fig. 5. Effects of N4Py and BnTPEN in PC-3 cells are reversed by pre-treatment with Zn. A: MTT assay; B: Western blot assay; C: Morphological changes. Treatment with iron alone (data not shown) resulted in similar effects as that with zinc alone. Concentrations and time points used: Fe and Zn = 100 μM, N4Py and BnTPEN = 10 μM. The 48 h metal pre-treatment, followed by 3 or 20 h co-treatment with ligand. [Color figure can be seen in the online version of this article, available at http://wileyonlinelibrary.com/journal/jcb]

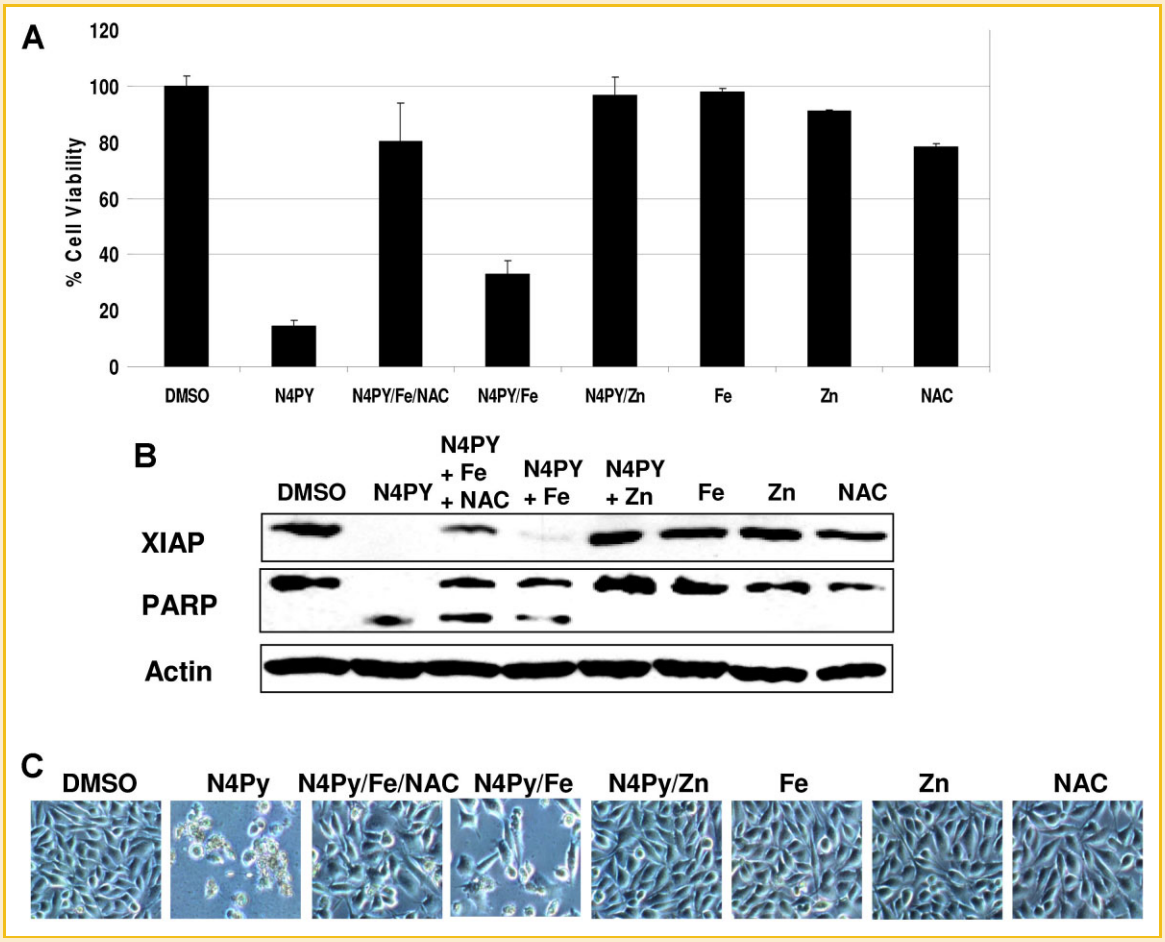

Fig. 6. Effects of N4Py are reversible by treatment with NAC. A: MTT assay; B: Western blot analysis; C: Morphological changes. Concentrations and time points used: NAC = 250 μM, Fe and Zn = 10 μM, N4Py = 5 μM, 20 h treatment. [Color figure can be seen in the online version of this article, available at http://wileyonlinelibrary.com/journal/jcb]

TREATMENT WITH *N*-ACETYLCYSTEINE (NAC) REVERSES N4Py-MEDIATED EFFECTS

To elucidate the possible mechanism by which Fe is able to only partially reverse N4Py-mediated effects as compared to full reversal by Zn, PC-3 cells were treated with 5 μmol/L of N4Py, 10 μmol/L of Fe or Zn, and 250 μmol/L of NAC. NAC is an inhibitor of ROS generation [Aruoma et al., 1989], which may occur in cells treated with Fe, which can redox cycle, but not in cells treated with Zn. When cell viability was measured by MTT assay, it was observed that treatment with NAC and Fe almost completely reversed the effects of N4Py, to a level comparable to those observed in cells treated with N4Py and Zn (Fig. 6A).

To further validate the effects of NAC addition, Western blot analysis was performed on PC-3 cell lysates after treatment with N4Py, Zn or Fe, and NAC. Interestingly, XIAP depletion by N4Py was partially reversed by NAC treatment, but PARP cleavage was not further reversed (Fig. 6B). The partial reversion of XIAP depletion may be due to the tighter binding of N4Py to Zn compared to Fe (77 times stronger), suggesting that Fe–N4Py may be able to strip Zn from XIAP to form a more potent cell death-inducing Zn–N4Py complex. Similarly, cell death associated morphological changes induced by N4Py were also partially reversed by addition of NAC (Fig. 6C). These results suggest that some Fe/N4Py-mediated cell death effects may be due to ROS generated through Fe redox cycling.

DISCUSSION

Zinc is a known enzyme inhibitor with a well-documented catalytic role in metalloenzymes, and the removal of Zn from the inhibitory enzymatic sites leads to increased enzyme activity [Maret et al., 1999]. However, in some RING-finger containing proteins, such as XIAP, it is well documented that Zn is important for structural stability of these enzymes, but the mechanism by which Zn-chelators induce XIAP depletion is not well-defined. One proposed mechanism suggests that depletion of full length XIAP may be a marker for cell death rather than a protective mechanism [Deveraux et al., 1999; Johnson et al., 2000; Levkau et al., 2001]. Therefore, this mechanism, as well as others by which the tested Zn-chelators induce apoptosis must be further investigated. In the current study, we have investigated this important mechanism by using a series of novel ligands with various Zn-binding abilities. We propose that

removal of Zn from the BIR-2 and -3 motifs by novel metal chelators like BnTPEN and N4Py destabilizes XIAP and causes breakdown of the enzyme, similar to the previously reported action of TPEN [Makhov et al., 2008]. Upon depletion of XIAP, caspases are consequently activated and cells undergo apoptosis (Fig. 7).

These chelators may also bind intracellular Fe, albeit with a lower affinity, but the Fe-binding ability of these compounds may also contribute to induction of cell death via an XIAP-independent pathway involving Fe redox cycling (Fig. 7). The interaction of these chelators with intracellular Fe and Fe-containing proteins must be examined. Importantly, other metals such as copper and cadmium may also bind to XIAP and induce conformational changes which are associated with destabilization of the enzyme [Mufti et al., 2006], suggesting that further exploration into possible interactions of these metals with the tested chelators is also necessary. Additionally, while other members of the IAP family contain Zn-binding RING finger motifs, less is known about the effect of metal chelation on these enzymes. This is a relationship that must be further elucidated. Finally, the mechanisms of action of these ligands found in cultured tumor cells should be confirmed in vivo in the future.

Because cancer cells have been shown to express high levels of XIAP, this may be a potential target for emerging therapeutics and while some success has been observed after treatment with small molecule XIAP inhibitors, recent studies have suggested a possibility for development of resistance to these inhibitors [Schimmer et al., 2006]. More recent reports also suggest important roles for XIAP in non-apoptotic pathways, such as NF-κB, MAPK, and the ubiquitin-proteasome pathway, which may have greater than previously anticipated effects on normal cellular processes [Srinivasula and Ashwell, 2008; Yang et al., 2009]. Therefore, the use of strong Zn-chelating compounds that induce depletion of XIAP may be a very promising strategy for the treatment of human malignancies.

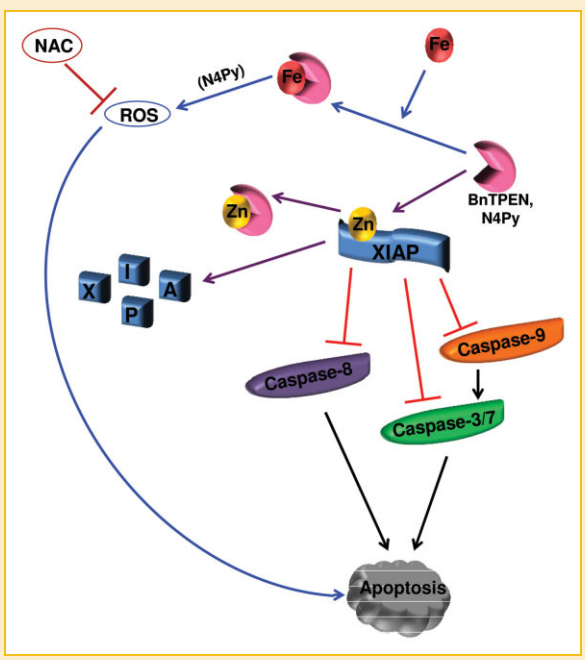

Fig. 7. Proposed mechanism by which Zn-chelators BnTPEN and N4Py induce cellular death. Zn-chelators with high Zn-binding affinity remove Zn from XIAP, causing degradation of the enzyme and ultimately leading to apoptotic cell death. Furthermore, the Fe-binding ability of these compounds may also contribute to induction of cell death via an XIAP-independent pathway involving Fe redox cycling.

ACKNOWLEDGMENTS

This work was partially supported by grants from Karmanos Cancer Institute 2009 Pilot Project Funding (to Q.P.D.) and the National Cancer Institute (1R01CA120009, 3R01CA120009-04S1, and 5R01CA127258-05, to Q.P.D.). J.J.K. thanks Wayne State University for its generous funding of this research.

REFERENCES

An B, Goldfarb RH, Siman R, Dou QP. 1998. Novel dipeptidyl proteasome inhibitors overcome Bcl-2 protective function and selectively accumulate the cyclin-dependent kinase inhibitor p27 and induce apoptosis in transformed, but not normal, human fibroblasts. Cell Death Differ 5:1062–1075.

Anderegg G, Hubmann E, Podder NG, Wenk F. 1977. Pyridine derivatives as complexing agents. XI. Thermodynamics of metal complex formation with bis-, tris- and tetrakis[(2-pyridyl)methyl]amines. Helv Chim Acta 60:123–140.

Aruoma OI, Halliwell B, Hoey BM, Butler J. 1989. The antioxidant action of *N*-acetylcysteine: Its reaction with hydrogen peroxide, hydroxyl radical, superoxide, and hypochlorous acid. Free Radic Biol Med 6:593–597.

Britovsek GJP, England J, White AJP. 2005. Non-heme iron(II) complexes containing tripodal tetradentate nitrogen ligands and their application in alkane oxidation catalysis. Inorg Chem 44:8125–8134.

Chai J, Shiozaki E, Srinivasula SM, Wu Q, Datta P, Alnemri ES, Shi Y. 2001. Structural basis of caspase-7 inhibition by XIAP. Cell 104:769–780.

Chang KL, Hung TC, Hsieh BS, Chen YH, Chen TF, Cheng HL. 2006. Zinc at pharmacologic concentrations affects cytokine expression and induces apoptosis of human peripheral blood mononuclear cells. Nutrition 22:465–474.

Chen D, Peng F, Cui QC, Daniel KG, Orlu S, Liu J, Dou QP. 2005. Inhibition of prostate cancer cellular proteasome activity by a pyrrolidine dithiocarbamate–copper complex is associated with suppression of proliferation and induction of apoptosis. Front Biosci 10:2932–2939.

Deveraux QL, Leo E, Stennicke HR, Welsh K, Salvesen GS, Reed JC. 1999. Cleavage of human inhibitor of apoptosis protein XIAP results in fragments with distinct specificities for caspases. EMBO J 18:5242–5251.

Duckett CS, Nava VE, Gedrich RW, Clem RJ, Van Dongen JL, Gilfillan MC, Shiels H, Hardwick JM, Thompson CB. 1996. A conserved family of cellular genes related to the baculovirus iap gene and encoding apoptosis inhibitors. EMBO J 15:2685–2694.

Duelund L, Hazell R, McKenzie CJ, Preuss Nielsen L, Toftlund H. 2001. Solid and solution state structures of mono- and di-nuclear iron(III) complexes of related hexadentate and pentadentate aminopyridyl ligands. J Chem Soc Dalton Trans 2001:152–156.

Eckelman BP, Salvesen GS, Scott FL. 2006. Human inhibitor of apoptosis proteins: Why XIAP is the black sheep of the family. EMBO Rep 7:988–994.

Franklin RB, Costello LC. 2009. The important role of the apoptotic effects of zinc in the development of cancers. J Cell Biochem 106:750–757.

Ghosh SK, Kim P, Zhang XA, Yun SH, Moore A, Lippard SJ, Medarova Z. 2010. A novel imaging approach for early detection of prostate cancer based on endogenous zinc sensing. Cancer Res 70:6119–6127.

Hashemi M, Ghavami S, Eshraghi M, Booy EP, Los M. 2007. Cytotoxic effects of intra and extracellular zinc chelation on human breast cancer cells. Eur J Pharmacol 557:9–19.

Huang H, Joazeiro CA, Bonfoco E, Kamada S, Leverson JD, Hunter T. 2000. The inhibitor of apoptosis, cIAP2, functions as a ubiquitin-protein ligase and promotes in vitro monoubiquitination of caspases 3 and 7. J Biol Chem 275:26661–26664.

Huang Y, Park YC, Rich RL, Segal D, Myszka DG, Wu H. 2001. Structural basis of caspase inhibition by XIAP: Differential roles of the linker versus the BIR domain. Cell 104:781–790.

Jackson C, Kodanko JJ. 2010. Iron-binding and mobilization from ferritin by polypyridyl ligands. Metallomics 2:407–411.

Johnson DE, Gastman BR, Wieckowski E, Wang GQ, Amoscato A, Delach SM, Rabinowich H. 2000. Inhibitor of apoptosis protein hILP undergoes caspase-mediated cleavage during T lymphocyte apoptosis. Cancer Res 60:1818–1823.

Levkau B, Garton KJ, Ferri N, Kloke K, Nofer JR, Baba HA, Raines EW, Breithardt G. 2001. XIAP induces cell-cycle arrest and activates nuclear factor-kappaB: New survival pathways disabled by caspase-mediated cleavage during apoptosis of human endothelial cells. Circ Res 88:282–290.

Liston P, Roy N, Tamai K, Lefebvre C, Baird S, Cherton-Horvat G, Farahani R, McLean M, Ikeda JE, MacKenzie A, Korneluk RG. 1996. Suppression of apoptosis in mammalian cells by NAIP and a related family of IAP genes. Nature 379:349–353.

Liston P, Fong WG, Korneluk RG. 2003. The inhibitors of apoptosis: There is more to life than Bcl2. Oncogene 22:8568–8580.

Makhov P, Golovine K, Uzzo RG, Rothman J, Crispen PL, Shaw T, Scoll BJ, Kolenko VM. 2008. Zinc chelation induces rapid depletion of the X-linked inhibitor of apoptosis and sensitizes prostate cancer cells to TRAIL-mediated apoptosis. Cell Death Differ 15:1745–1751.

Maret W, Jacob C, Vallee BL, Fischer EH. 1999. Inhibitory sites in enzymes: Zinc removal and reactivation by thionein. Proc Natl Acad Sci USA 96:1936–1940.

Mufti AR, Burstein E, Csomos RA, Graf PC, Wilkinson JC, Dick RD, Challa M, Son JK, Bratton SB, Su GL, Brewer GJ, Jakob U, Duckett CS. 2006. XIAP is a copper binding protein deregulated in Wilson's disease and other copper toxicosis disorders. Mol Cell 21:775–785.

Murakami M, Hirano T. 2008. Intracellular zinc homeostasis and zinc signaling. Cancer Sci 99:1515–1522.

Provinciali M, Di Stefano G, Fabris N. 1995. Dose-dependent opposite effect of zinc on apoptosis in mouse thymocytes. Int J Immunopharmacol 17:735–744.

Roelfes G, Lubben M, Leppard SW, Schudde EP, Hermant RM, Hage R, Wilkinson EC, Que L, Jr., Feringa BL. 1997. Functional models for iron-bleomycin. J Mol Catal A Chem 117:223–227.

Rothe M, Pan MG, Henzel WJ, Ayres TM, Goeddel DV. 1995. The TNFR2–TRAF signaling complex contains two novel proteins related to baculoviral inhibitor of apoptosis proteins. Cell 83:1243–1252.

Schimmer AD, Dalili S. 2005. Targeting the IAP family of caspase inhibitors as an emerging therapeutic strategy. Hematol Am Soc Hematol Educ Program 2005:215–219.

Schimmer AD, Dalili S, Batey RA, Riedl SJ. 2006. Targeting XIAP for the treatment of malignancy. Cell Death Differ 13:179–188.

Shiozaki EN, Chai J, Rigotti DJ, Riedl SJ, Li P, Srinivasula SM, Alnemri ES, Fairman R, Shi Y. 2003. Mechanism of XIAP-mediated inhibition of caspase-9. Mol Cell 11:519–527.

Srinivasula SM, Ashwell JD. 2008. IAPs: What's in a name? Mol Cell 30:123–135.

Sun C, Cai M, Meadows RP, Xu N, Gunasekera AH, Herrmann J, Wu JC, Fesik SW. 2000. NMR structure and mutagenesis of the third Bir domain of the inhibitor of apoptosis protein XIAP. J Biol Chem 275:33777–33781.

Suzuki Y, Nakabayashi Y, Nakata K, Reed JC, Takahashi R. 2001a. X-linked inhibitor of apoptosis protein (XIAP) inhibits caspase-3 and -7 in distinct modes. J Biol Chem 276:27058–27063.

Suzuki Y, Nakabayashi Y, Takahashi R. 2001b. Ubiquitin-protein ligase activity of X-linked inhibitor of apoptosis protein promotes proteasomal degradation of caspase-3 and enhances its anti-apoptotic effect in Fas-induced cell death. Proc Natl Acad Sci USA 98:8662–8667.

Tang H, Arulsamy N, Radosz M, Shen Y, Tsarevsky NV, Braunecker WA, Tang W, Matyjaszewski K. 2006. Highly active copper-based catalyst for atom transfer radical polymerization. J Am Chem Soc 128:16277–16285.

Uren AG, Pakusch M, Hawkins CJ, Puls KL, Vaux DL. 1996. Cloning and expression of apoptosis inhibitory protein homologs that function to inhibit apoptosis and/or bind tumor necrosis factor receptor-associated factors. Proc Natl Acad Sci USA 93:4974–4978.

Wong Y-L, Mak C-Y, Kwan HS, Lee HK. 2010. Mononuclear iron(III) complexes supported by tripodal N3O ligands: Synthesis, structure and reactivity towards DNA cleavage. Inorg Chim Acta 363:1246–1253.

Yang Y, Fang S, Jensen JP, Weissman AM, Ashwell JD. 2000. Ubiquitin protein ligase activity of IAPs and their degradation in proteasomes in response to apoptotic stimuli. Science 288:874–877.

Yang H, Zonder JA, Dou QP. 2009. Clinical development of novel proteasome inhibitors for cancer treatment. Expert Opin Investig Drugs 18:957–971.